



HAL
open science

Failure of Arrhenius plots for investigation of localized levels

R. Ongaro, A. Pillonnet

► **To cite this version:**

R. Ongaro, A. Pillonnet. Failure of Arrhenius plots for investigation of localized levels. *Revue de Physique Appliquée*, 1990, 25 (2), pp.209-227. 10.1051/rphysap:01990002502020900 . jpa-00246180

HAL Id: jpa-00246180

<https://hal.science/jpa-00246180>

Submitted on 4 Feb 2008

HAL is a multi-disciplinary open access archive for the deposit and dissemination of scientific research documents, whether they are published or not. The documents may come from teaching and research institutions in France or abroad, or from public or private research centers.

L'archive ouverte pluridisciplinaire **HAL**, est destinée au dépôt et à la diffusion de documents scientifiques de niveau recherche, publiés ou non, émanant des établissements d'enseignement et de recherche français ou étrangers, des laboratoires publics ou privés.

Classification
 Physics Abstracts
 72.20H

Failure of Arrhenius plots for investigation of localized levels

R. Ongaro and A. Pillonnet

Laboratoire d'Electricité, Université Claude Bernard, 43 Boulevard du 11 Novembre 1918, 69622 Villeurbanne Cedex, France

(Reçu le 1^{er} décembre 1988, révisé le 19 octobre 1989, accepté le 27 octobre 1989)

Résumé. — L'étude de l'ionisation Poole Frenkel, lorsque les niveaux localisés sont distribués en bandes, est réalisée en prenant la température T comme variable. Un grand nombre de simulations a révélé le même comportement qualitatif des diagrammes d'Arrhénius de la conductivité ($\log \sigma$, $1/T$), que celui présenté par un seul niveau. De nombreux exemples sont traités, pour montrer clairement que des portions linéaires étendues peuvent être obtenues sur les courbes, quelle que soit la largeur de la distribution. En conséquence, les énergies d'activation, déduites de ces diagrammes, ne peuvent plus être assignées à un niveau d'énergie réel quelconque. Nous croyons avoir montré que, poser comme principe que les niveaux d'un système à niveaux multiples peuvent toujours être séparés en leurs composantes, est en contradiction avec la statistique de Fermi-Dirac.

Abstract. — Investigation of Poole Frenkel ionization, when the localized levels are distributed within bands, is realized with temperature T as the variable. A large amount of simulations revealed the same qualitative behaviour of Arrhenius diagrams of conductivity ($\lg \sigma$, $1/T$), as that given by a single level. Many examples are treated, in order to make clear that extended linear parts can be obtained, as wide as the distribution can be. Consequently, the activation energies deduced from these diagrams can no more be assigned to any actual localized level. We believe to have shown that setting down as a principle that levels, in a multi-level system, can always be splitted into their components, is in contradiction with Fermi-Dirac statistics.

1. Introduction.

Arrhenius diagrams were used for many decades as a very simple means allowing for determination of activation energies. Their field of application is extremely varied. However, for the present purpose, we have limited the analysis to the investigation of energy levels located into the gap of solids. Moreover, in this area, we restrict further the matter to representations of conductivities in terms of T^{-1} , when an applied field is supposed to be the only source of perturbation of thermal equilibrium. Nevertheless, the domain of applicability of our study remains quite large, as it encompasses all the analyses of currents against temperature, where bulk conduction mechanisms dominate, such as, for instance, Poole-Frenkel (PF) effect. It includes also the analysis of energy levels in the gap, by the thermally-stimulated-current (TSC) method.

The use of such diagrams is simple for, when the measured entity is expected to vary following an exponential form, $y \propto \exp(-W/kT)$, it would give

a straight line in a $(\lg y, 1/T)$ plot. In addition, another simple idea is associated with such a graph : if several energies W_i are assumed, then, the same entity y would appear as a sum of exponential contributions. In an Arrhenius plot, a curve displaying a continuously varying slope obtains then. Consequently, it can be theoretically splitted into a few straight lines. This would be the case, for example, for the model analysed by Mott and Davis [1], which is given as representative of three main types of superimposed conductivities in amorphous materials (see sub-section 2 below). Such splitting corresponds, besides, to the fact that, from a strict mathematical point of view, a great wealth of continuous curves can be approached by a series in exponential terms. This is why some authors like Gardner *et al.* [2], and then, especially, Provencher [3], put into shape more and more sophisticated mathematical technics to determine the parameters of each component. Similarly, the technic of TSC appears, mainly, as a direct experimental method of splitting off the exponential components. Let us recall that it consists, sometimes, in resolving the

current into its various components, by a series of successive temperature rises with increasing maxima, each followed by a lowering-back to the initial temperature.

Thence, the use of Arrhenius plots seems to lie on an apparently common sense principle, which we call, for the sake of convenience, « splittability principle ». If this principle were always working, the various contributions to the conductivity, of levels with different energies, would always be expressible through a sum of exponential terms. Each of these terms seems then to proceed readily from Boltzmann function. So that, this principle establishes a bi-univocal correspondence, between a set of conductivity components, and an any shaped distribution of localized states in the gap, which occupation rates would follow Boltzmann statistics. Therefore, the splittability principle, appearing as fully legitimate, from either physical or mathematical view-points, has practically never been suspected. As a result, the Arrhenius plot is universally considered as a well-behaved tool, succeeding very simply in the investigation of flaws in the gap of materials.

Examples are so many, showing up the very large agreement of searchers about this, that any significant inventory is impossible. Just in order to give one example in the field of crystalline solids, Fritzsche [4] can be cited. This author finds that the n-type conductivity of Ge doped with Sb, is representable by a set of three straight lines, from which he deduces three trap levels. More recently, the same kind of analysis has been applied, as a rule, to amorphous materials. We adopted ourselves the same attitude in analysing currents in the amorphous chalcogenide $\text{As}_{35}\text{Te}_{28}\text{Ge}_{16}\text{S}_{21}$ (Felix *et al.* [5]), or in α -PVDF (Felix-Vandorpe *et al.* [6]). Conversely, many authors have contrived models with N localised levels, in order to interpret some typical variations of currents with temperature. The models of Cohen, Fritzsche and Ovshinsky [7], or of Davis and Mott [8], can be cited as examples, in the field of amorphous semiconductors.

This brief recall gives an idea of the upsetting, any challenge of the validity of Arrhenius plots, as a proof of the actual existence of some kind of level distribution in the gap of materials, would introduce into the practice of experimental, as well as theoretical, analyses. Now, we have developed, in two preceding papers [9, 10], an exact formulation of models with one donor level only, or with donors distributed in energy. With the help of computer simulation, we have been able to compare curves obtained in either case, when F is varied. It remains presently, to simulate the corresponding temperature variations. This will afford us convincing arguments, against the general effectiveness of the splittability principle.

2. Survey of possible forms of $\sigma(T)$.

Before analysing the influence of an energetic distribution of donors, on the shape of the conductivity $\sigma(T)$, let us recall briefly, the most common relationships between $\sigma(T)$ and the density $n(T)$ of free electrons. If electrons are the dominant carriers, the general relationship between $\sigma(T)$ and $n(T)$ can be written simply :

$$\sigma(T) = C(T) n(T) \quad (1)$$

$C(T)$ being a convenient parameter, eventually independent of T . This equation shows that the effective shape of curves, in an Arrhenius plot, depends upon the form adopted for $C(T)$.

When crystalline semiconductors are concerned, the pre-exponential factor in (1) writes :

$$C(T) N_c(T) = e\mu(T) N_c(T) = eK_c \mu(T) T^{3/2} \quad (2)$$

N_c being the density of states in the conduction band. Then, its variation against T is that of the function $\mu(T) T^{3/2}$. Many theoretical forms of $\mu(T)$ are available in literature. However, as we are interested mostly with the possible influences of $\mu(T)$ on graphical representations, we shall not attempt an exhaustive account of these forms, and of the relevant physical background. For that references [11] or [12] can be consulted. To indicate simply an approximate panel of forms, $\mu(T)$ can be taken roughly as proportional : to $T^{-3/2}$ when carriers are diffused by acoustical phonons ; to T^0 when nearly temperature independent behaviour results from scattering by neutral impurities ; or to T when diffusion by dislocations is dominant ; or to $T^{3/2}$ when scattering proceeds from charged impurities. In addition, proportionality to $T^{-7/3}$ or $T^{-5/3}$ have been derived, respectively in p-Ge and n-Ge, when scattering results from interactions with optical or intervalley phonons. As a matter of fact, much intricate forms are actually derived.

The different processes may act simultaneously, and the resulting mobility is, actually, a very intricate function of T . However, in so far as processes can be considered as independent, the resulting reciprocal mobility is often taken as a sum over the reciprocal mobility components. Therefore, when the contributing terms are reduced to power functions

$$\mu^{-1} = \sum_i A_i T^{-b_i} \quad (3)$$

Following Conwell, it should be better summing the reciprocal relaxation times before deriving the equivalent mobility.

When amorphous materials are concerned, two types of conduction can be relevant, either in the extended states of the conduction band, or in some kind of localized states in the gap. Therefore, in

equation (1), the expression for $C(T)$ must be specified, following both the kind of assigned conductivity, and the pertinent theoretical model. Equation (2) can be used to describe conduction in the extended states, if $N(E_c)$ is substituted for N_c . Actually, the problem of conductivity is, more often, approached directly through a consideration of few exponential contributions (see e.g. Mott and Davis, [1]):

$$\sigma = \sum_i C_i \exp\left(-\frac{W_i}{kT}\right). \quad (4)$$

For instance, in the model of Davis and Mott [8], three components are mainly postulated. In the high temperature range, conduction should be due to an excitation of carriers, beyond the mobility shoulder, into non-localized states. In the intermediate range, conductivity should proceed from carriers excited into localized states of the conduction band tail. At weaker temperatures, a hopping conduction, through nearest neighbour sites, prevails in localized states close to the Fermi level. This latter process is analogous to the conductivity in an impurity band, for a heavily doped crystal. Moreover, in a still weaker temperature range, carriers should hop directly into more distant sites. This is the well-known model of Mott [13], in which σ becomes proportional to $\exp(-BT^{-1/4})$.

Moreover, it can be remarked that, in amorphous solids where disorder is an important source of scattering, there does not seem to exist so sophisticated theories of mobility as in semiconductors. Therefore, expressions of the pre-exponential factors in (4) appear rather as rule of thumb formulations. For example (see Mott and Davis [1], p. 201), it can be shown that, for the high temperature range, $C_1 \propto \mu T$, and $\mu \propto T^{-1}$. This description is hardly modified when mobility is activated. Because, then, the exponential factor, would contribute to the overall activation energy.

Various other mobility laws can be cited. Among them, let us indicate the mobility resulting from collisions of phonons with large or small polarons. Following Howard and Sondheimer [14], mobility can be written, in the former case, either as $\mu_{lp} \propto T^{1/2}$, in the high temperature range; or as

$$\mu_{lp} \propto T^{1/2} G(T) \left(\exp\left(\frac{\hbar\omega}{kT}\right) - 1 \right),$$

at low temperature. $G(T)$ is a slowly varying func-

tion of T , close to 1. A slightly different form obtains when phonons and polarons are tightly coupled. When small polarons are concerned, the Holstein's model [15] leads to a very involved relation, which takes the approximate form:

$$\mu_{sp} \propto T^{-3/2} \exp\left(-\frac{\gamma \hbar\omega}{2kT}\right)$$

in the high temperature range, γ being a coupling parameter.

Finally, it appears that so many mobility functions are available that choosing the right one, in interpreting a given set of data, is not always easy, especially in non-crystalline materials. This could be why Arrhenius representations are very often taken simply as $(\lg j, 1/T)$ plots. The incidence of this choice will be estimated in section 3.2 below.

3. Non-splittability of levels, in a uniform band.

Developments in [9] and [10] were devoted to the analysis of curves obtained, at constant temperature under the influence of a field, either when one level only exists, or when donors are distributed in energy. The related behaviours, in terms of temperature variations, can then be deduced readily. For this purpose, it is only needed to precise the form of $C(T)$.

If crystalline solids are considered, $\sigma = e\mu N_c n_r$, then in equations (5) of [9], the multiplying factor sN_c is independent of temperature. This means that curves for which $\sigma(T) \propto n(T)$, with $\mu = \mu_1$ independent of T , are given by the Arrhenius plot $(\lg(n_r T^{3/2}), 1/T)$. If now, mobility is supposed to vary following a given power of T , say $\mu = \mu_2 T$ or $\mu = \mu_3 T^{-3/2}$, the related plots, to be simulated, would be respectively, $(\lg(n_r T^{5/2}), 1/T)$ and $(\lg n_r, 1/T)$.

More generally, anyone of the forms of $\mu(T)$ or $C(T)$ quoted above, must be related to an appropriate Arrhenius plot, with the proper function $\lg(n_r F(T))$ as ordinate.

3.1 VARIATIONS OF $T^{3/2} n_r(T)$ (CONSTANT MOBILITY). — The main purpose of the present study, is to compare the curves given by the one-donor-level model, to that given by the uniform distribution of donors in energy.

3.1.1 One-donor-level case. — This case is treated readily by simulation of equation (5b) of [9], multiplied by $T^{3/2}$, namely:

$$n_r T^{3/2} = \frac{2 s T^{3/2} q - 1}{q} \left(\left(1 + \frac{s}{q} e^{(\eta - \alpha_p)} \right) \left(\sqrt{1 + 4 s \frac{q-1}{q} \frac{e^{\eta - \alpha_p}}{\left(1 + \frac{s}{q} e^{\eta - \alpha_p} \right)^2} + 1} \right) \right) \quad (5)$$

with T as the variable, and for various, constant, applied fields, and $sT^{3/2}$ being independent of T . In this equation $\eta = \Phi/kT$ is the relative well depth, $\alpha_p = \Delta\Phi_p/kT$ the relative field-induced potential lowering for an any shaped well, $s = N_d/N_c$ and $q = N_d/N_a$, N_d and N_a being respectively the densities of donors and acceptors.

The related Arrhenius plot is represented in figure 1, with the limits in temperature 100 K and 573 K. To emphasize the influence of the applied field on the shape of curves, the relative barrier lowering $\Delta\Phi_p/\Phi$ was given three values : 0.3 ; 0.65 and 0.85. These define three families of curves, characterized by suitable s and q values. In each family, q is varied by powers of 10, from 1.04 to

10^5 . Moreover, in families 1 and 3, $s_{\max} = s(100\text{ K})$ equals either 10^{-1} or 10^{-6} ; in family 2, $s_{\max} = 10^{-6}$ only. Two main observations can be made about these curves. First, it appears that they can display more or less extended quasi-linear parts, corresponding to the slope parameters $m = 1$ or $m = 2$, as usual in α_p plots. Thus, as it could be inferred easily, the Arrhenius plot of the one-level model, is made up of two straight lines, contrary to the statements of the splittability principle. Secondly the slope of curves depends upon the value to which the saturation ratio $\Delta\Phi_p/\Phi$ is amounting. A distortion of curves, drawn for the same s and q values, results from an increase in this ratio; namely, the curves are stretched along, as if the $1/T$ scale was

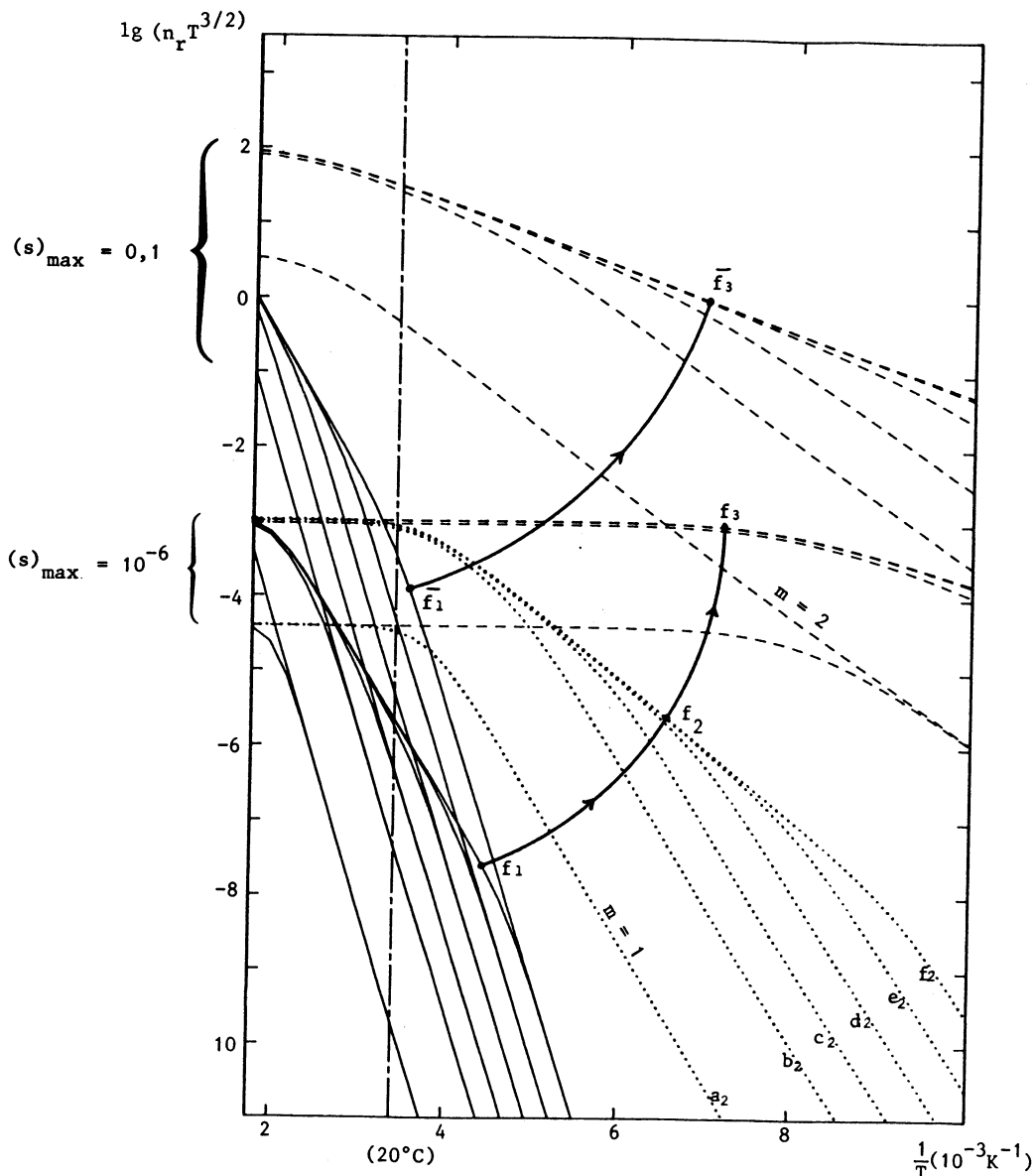


Fig. 1. — Variations of $\lg(n_r T^{3/2})$ versus $1/T$ in a one-level model, for various values of the saturation ratio $\Delta\Phi_p/\Phi$. $\Phi = 1\text{ eV}$. $\Delta\Phi_p/\Phi$: --- 0.3 ; $\text{-}\cdot\text{-}\cdot\text{-}$ 0.65 ; $\text{-}\cdot\text{-}\cdot\text{-}\cdot\text{-}$ 0.85. Letters a_i to f_i (indicated only for family 2) correspond to $s_{\max} = 10^{-6}$ and to the q values : 1.04, 10.4, 104, 10^3 , 10^4 , 10^5 . Curves \bar{f}_i correspond to $s_{\max} = 0.1$.

expanded. To give some examples, the quoted growth in $\Delta\Phi_p/\Phi$ makes curve f_1 to transform successively into curves f_2 and f_3 . The same is true for curves \bar{f}_1, \bar{f}_3 (see circular arrows in the Fig.).

This result shows that, when the field approaches its maximum F_s , conductivity becomes a slightly varying function of T , even in an extended interval. Comparison of curves f_3 and \bar{f}_3 shows, in addition, that this phenomenon manifests itself the more easily, the weaker the density of donors. In such a case, an experimentalist would certainly not try to promote a PF mechanism, as an available interpretation of his data. For, Boltzmann function does not bring any possibility to put together an invariance of $\sigma(T)$ with a PF regime.

3.1.2 Uniform distribution of donors. — This case needs to compute equation (4) of [10], namely :

$$n_r + \frac{s}{q} = \frac{s}{\delta\eta} \ln \frac{e^{-(\eta_1 - \alpha_p)} + n_r}{e^{-(\eta_2 - \alpha_p)} + n_r} \quad (6)$$

with $\eta_1 = \Phi_1/kT$ and $\eta_2 = \Phi_2/kT (\Phi_2 > \Phi_1)$.

Let us recall that this relationship describes typically transitions between conduction band and trapping levels, perturbations of thermal equilibrium by the applied field being accounted for through the existence of a steady-state Fermi level [16]. Hence, direct transitions through the levels are considered as very improbable. Likewise, impact ionization by hot electrons is not taken into consideration, in conformity with a usual prerequisite of PF theories.

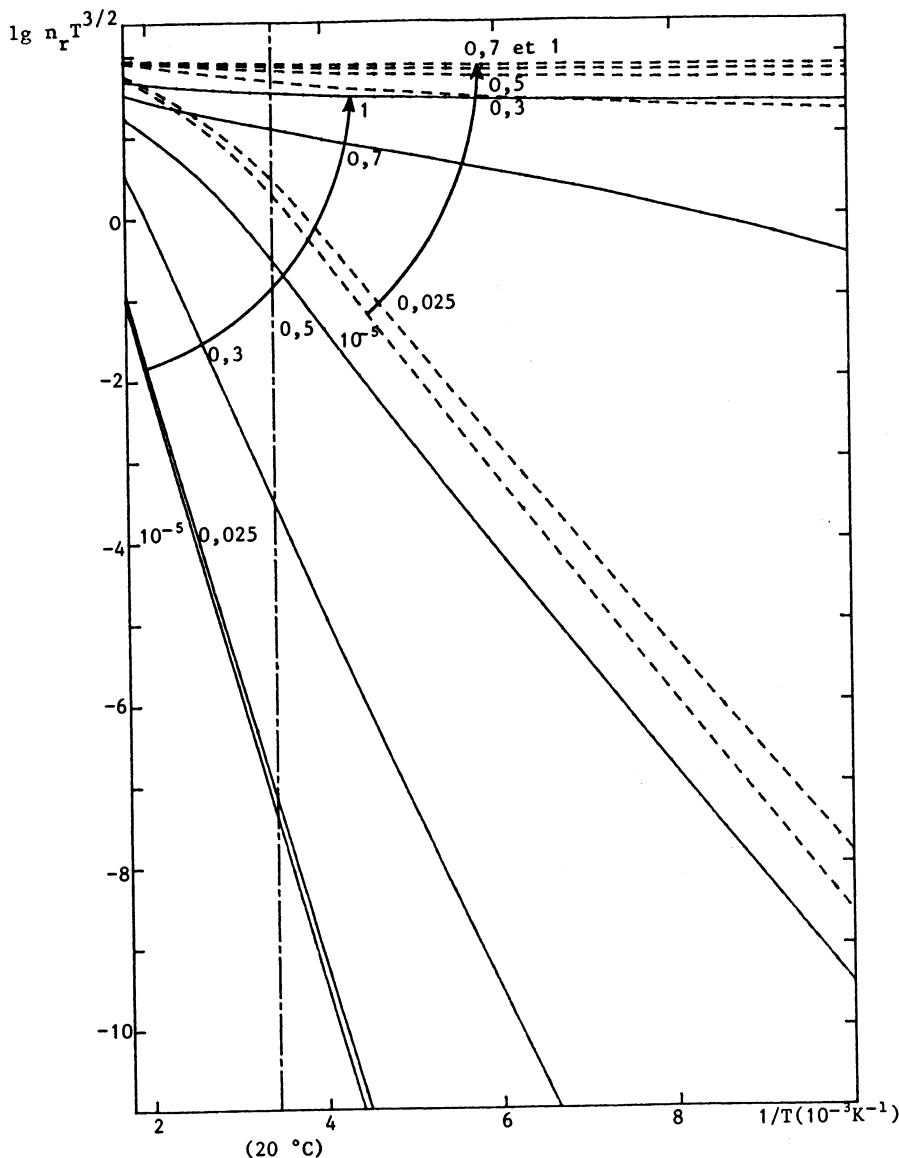


Fig. 2. — Variations of $\lg(n_r T^{3/2})$ versus $1/T$ for a uniform band, showing the influence of $\delta\Phi$ for two saturation ratios. $\Phi_2 = 1$ eV ; $s_{max} = 0.1$; $q = 10.4$. $\Delta\Phi_p/\Phi_2$: family (1) $\frac{0.30}{\dots}$; family (2) $\frac{0.75}{\dots}$. $\delta\Phi$ values (in eV) are indicated on curves.

Some examples of $\lg(n_r T^{3/2})$ variations against $1/T$, are plotted in figures 2, 3a and 3b, to show what kind of behaviour can result when a uniform distribution of donors is concerned. The model is not otherwise different from the model of sub-section 3.1.1 above. However, it introduces one more parameter, the band-width $\delta\Phi$. Moreover, the saturation ratio is now necessarily defined as $\Delta\Phi_p/\Phi_2$, Φ_2 being the maximum donor depth (see [10], Fig. 1).

It is observed mainly that, despite the widening of the distribution, the same quasi-linear parts are still present on the curves, corresponding to the same

slope parameter values, $m = 1$ and $m = 2$. A careful examination of these parts shows, however, that slightly more visible bending, physically insignificant, results from band widening.

Figure 2 is made up of two families of curves, labelled (1) and (2) and corresponding to the $\Delta\Phi_p/\Phi_2$ values, 0.30 and 0.75. In each family, $\delta\Phi$ (in eV) is given the following values: 10^{-5} (very close to one level); 2.5×10^{-2} ; 0.30, 0.50, 0.70 and 1 (full band). For the sake of easiness in comparing figures 1 and 2, $\Phi_2 = 1$ eV, $s_{\max} = 0.1$ and $q = 10.4$. It is observed that, when the system is going from the quasi-unique level case, to the case of a

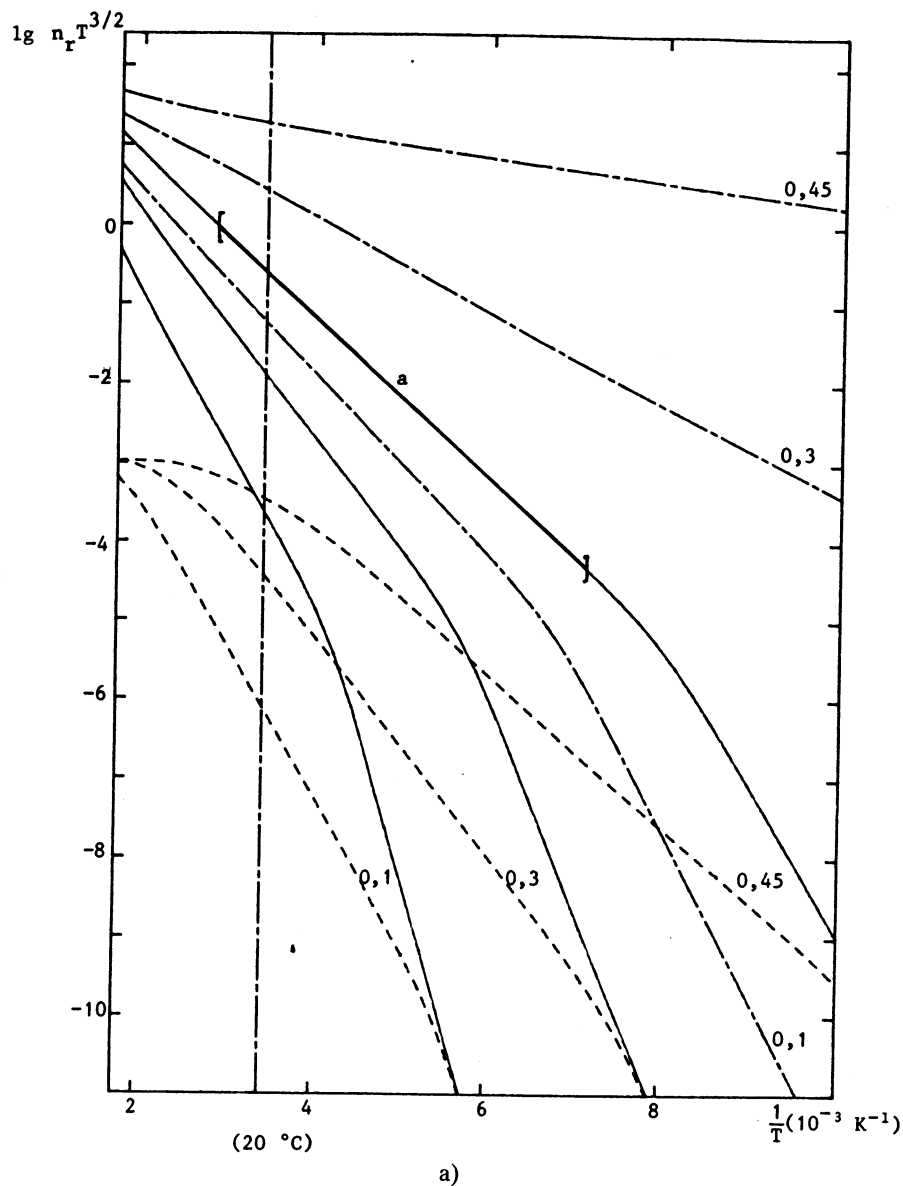


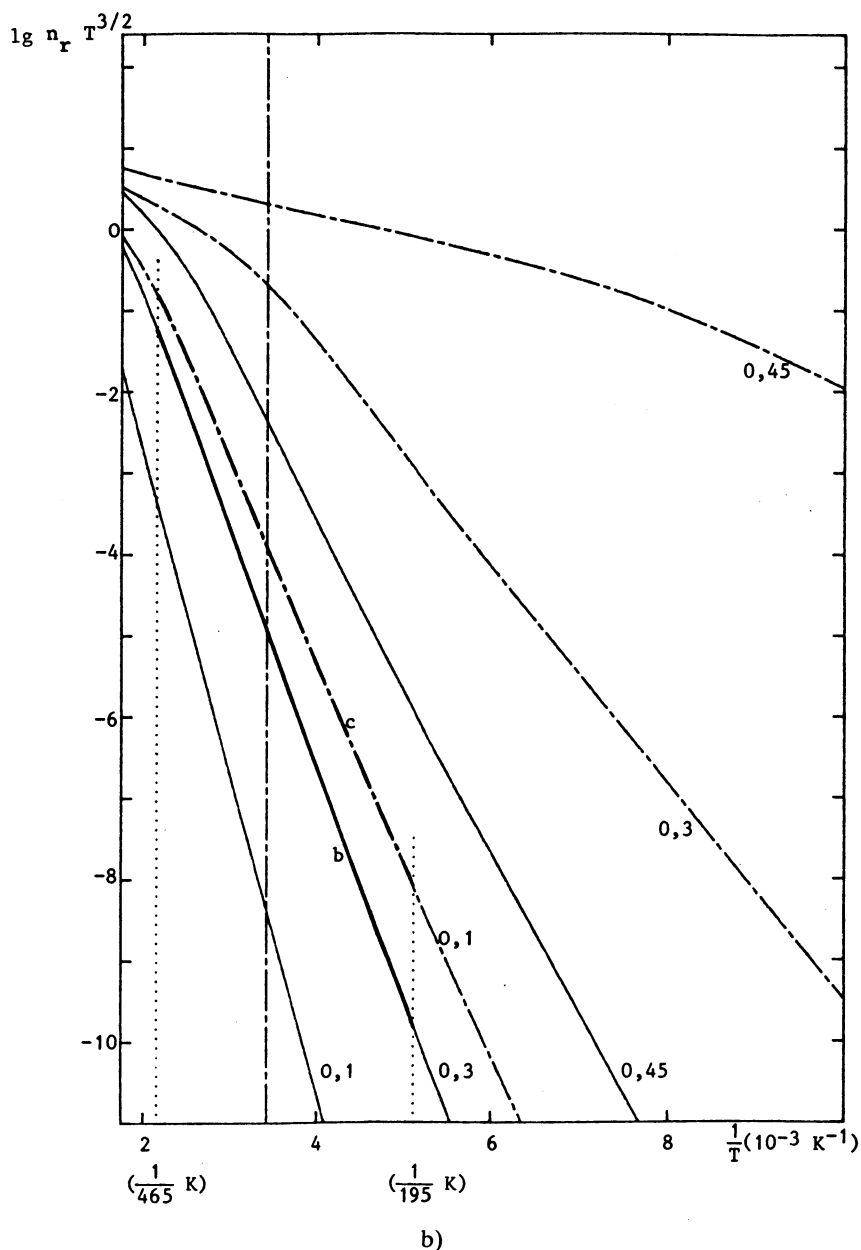
Fig. 3. — $\lg(n_r T^{3/2})$ versus $1/T$ for a uniform band, showing the influence of $\Delta\Phi_p/\Phi_2$ for various $\delta\Phi$. $\Phi_2 = 1$ eV. Values of $\Delta\Phi_p/\Phi_2$ are indicated on curves. (a) $q = 10^7$. Family (3): $s_{\max} = 0.1$; $\delta\Phi = 0.2$ eV (—); family (4): $s_{\max} = 0.1$; $\delta\Phi = 0.5$ eV (---); family (5): $s_{\max} = 10^{-6}$; $\delta\Phi = 0.2$ eV (- - - - -). []: Limits within which curve a is quasi-linear. (b) $q = 10.4$ and $s_{\max} = 10^{-2}$. Family (6): $\delta\Phi = 0.2$ eV (—); family (7): $\delta\Phi = 0.5$ eV (---).

complete band, the slopes of curves decrease steadily (see circular arrows in the Fig.), and become very small for $\delta\Phi = 1$ eV. Therefore, a progressive widening of the band of donors, from Φ_2 upwards, appears mostly, as equivalent to a field enhancement in the one-level case. Two more observations can be made, from a comparison of curves of families (1) and (2). First, the range of slope variations is the larger, the smaller $\Delta\Phi_p/\Phi_2$. Secondly, the slope sensitivity to small $\delta\Phi$ variations, in narrow bands, increases with $\Delta\Phi_p/\Phi_2$. For example, in family (1), the curves corresponding to $\delta\Phi = 10^{-5}$ eV and $\delta\Phi = 2.5 \times 10^{-2}$ eV merge in, whilst, in family (2), the same curves are significantly far apart.

These topics are easily interpretable. Because, for any given field strength, the amount of empty levels tends to increase with the band width. In the case of

relatively narrow bands, especially, a high value of $\Delta\Phi_p/\Phi_2$ implies that the deeper empty level is close to Φ_2 . Thus, a small increase in $\delta\Phi$, at constant N_d , leads to a new repartition, containing more empty levels, namely those levels which have reached the saturation condition.

Figure 3a shows the Arrhenius plot which obtains when $\Delta\Phi_p/\Phi_2$ is varied, for two given (constant) widths of the donor band ($\delta\Phi = 0.2$ eV for families (3) and (5); $\delta\Phi = 0.5$ eV for family (4)). In each family, the saturation ratio takes the values: 0.1, 0.3 and 0.45; $\Phi_2 = 1$ eV; $s_{\max} = 0.1$ except for family (5) where $s_{\max} = 10^{-6}$; and $q = 10^7$ (no compensation at all). These curves have been drawn to exemplify cases where the curves display two quasi-linear parts ($m = 1$ and $m = 2$). It is apparent in the figure, that the quasi-linear portions are liable to



extend over quite large temperature intervals. In curve (a), for example, a convenient linearity extends over a temperature range lying, at a minimum, between 140 K and 350 K. The corresponding σ variation is then of about 4.5 decades. Now, this interval is rather reduced, owing to the assumption of non-compensation ($q = 10^7$).

Therefore, figure 3b was drawn to give an idea of the ranges of linearity that can be achieved, when a significant compensation is postulated ($q = 10.4$). Then, curves (b) and (c) for example, can be considered as straight lines, with an excellent approximation, at least over a temperature interval going from 195 K to 465 K. The related variations of σ extend, respectively, over 9 and 7.5 decades. These ranges are so large that they may encompass a great deal of experimental data. So that our model could bring a theoretical background to the so-called Stuke rule (Stuke, [17]), following which extended linear Arrhenius plots are often found in amorphous glasses.

3.1.3 Concluding remarks. — The above developments have put forward that the fact of finding straight lines, in an Arrhenius plot, does not bring any proof element about the actual distribution of traps, in the gap of materials. Because it was shown that one or two levels can be found, either when one level only is stated, or when levels are distributed within a band, as wide as it can be. Therefore, this implies a failure of the analyses based upon Arrhenius plots. It must be noted that some authors have sometimes conjectured a non universal availability of the splittability principle. For example, Connell *et al.* [18] made some reservations about it. They remark, particularly, that a single activation energy is often found in amorphous semiconductors, though more or less extended distributions of localized states are generally admitted, in the gap of these materials. These authors have then shown, through a calculation initially nearly ours, that it is possible to find a unique activation energy, when a narrow band of uniformly distributed centres is stated. However, as their calculation lies on a first order approximation, their result could not, fundamentally, point out a significant irrelevance of Arrhenius plots.

Finally, it remains desirable to widen the present study in three directions. The first is to examine how much other forms of mobility can affect the observed linearities. The second is to see what kind of $\sigma(1/T)$ curves result from the consideration of a set of discrete levels. The third is to try to explain why the splittability principle does not work, in our models.

3.2 ARRHENIUS PLOTS FOR $T^q n_r$ TYPE VARIATIONS. — The preceding $n_r(1/T)$ representation is

a little restraining, as it would correspond only to a diffusion by neutral impurities. Such a diffusion mechanism can hardly be envisaged in our models, with donors and acceptors present, except in the lowest temperature range, and for small applied fields.

To simulate the most general case, a form like (3) should be used, but it would imply an arbitrary choice of the parameters A_i . Therefore, it seemed preferable, instead, to draw examples of the individual effects of some of the components in (3). This can be achieved readily, by giving relevant values to b , $b = b_i + \frac{3}{2}$ being the exponent to be used for μ when a T^{b_i} power law is adopted, in order to ensure that the parameter factorized in conductivity equations be independent of T . Three cases of mobility are considered, namely : diffusion by acoustic phonons, which obtains with $b = 0$; diffusion by dislocations, corresponding to $b = 5/2$, this case being generally that of amorphous semiconductors ; and diffusion by charged impurities, which is given by $b = 3$.

(i) Figure 4 was drawn with the only purpose of showing the deformations undergone by curves (a) and (c) of figures 3a and 3b, when $\mu(T)$ is changed. Conductivities are given in arbitrary units, the various curves being translated along the ordinate axis, in order to make them to coincide at point A ($T = 100$ K). It is observed, of course, that a growth in curve steepness results from an increase in b . But, it is important to notice that curves are still displaying extended quasi-linear parts. When a straight line fitting is realized at the best, particularly for the high temperature side of the (a)-type curves, these lines converge towards a common point A'. This convergence is obvious. Because the pre-exponential factor gives, in the diagram, a straight-line of equation $-b \lg(1/T)$, which added to the curve $n_r(T)$ results, principally, in a rotation according to the variations of b . Besides, figure 4 shows, very generally, that the assumptions made about the function $C(T)$, entail some degree of undetermination, for the activation energies deduced from the slopes, after the splittability principle (maximum discrepancy of the order of 7 %, at a maximum, in the temperature range used). This evident assertion does not seem to be always stated with sufficient care in literature.

We have tabulated, in table I, the various activation energies that an experimentalist would deduce from figure 4.

This table establishes that the weaker energies $*\Phi_1$, found from type (a) curves, are fully irrelevant. Besides, if an experimentalist supposed these values to correspond to $m = 2$, he could not find more adequacy with the ranges of energies involved in the model. For the deeper levels, deduced from curves (a) and (c), the obtained energies belong to the

Table I.

	Curves	a ₁	a ₂	a ₃	a ₄	c ₁	c ₂	c ₃	c ₄
Measured	*Φ ₁ (eV)	0.62	0.64	0.66	0.67				
	*Φ ₂ (eV)	0.82			0.85	0.90	0.93	0.96	0.97
Model		0.8 ≤ Φ ≤ 1 eV				0.5 ≤ Φ ≤ 1 eV			

ranges of energies stated in the model. However, it must be remarked that, for curves (a), the measured energies *Φ₂ are very close to the top of the band (0.80 ≤ Φ ≤ 1 eV), whilst, for curves (c), they range near the bottom of the band, despite a larger

spreading of levels (0.5 ≤ Φ ≤ 1 eV). This is directly related to the compensation ratio. For, when no compensation exists (q = 10⁷ for curves (a)), all levels in the band are rather largely occupied. But, when a significant compensation is achieved (q = 10.4 for curves (c)), the shallower levels are largely emptied, and conductivity is mostly contributed for the deeper sites.

(ii) As an illustration, and to make this more prominent, we have represented in figure 5 the rate of level occupation

$$a_r = \frac{1}{N_c} \frac{d(N_d - n_d)}{d\Phi} = \frac{A_r}{1 + n_r^{-1} \exp\left(-\frac{\Phi - \Delta\Phi_p}{kT}\right)}$$

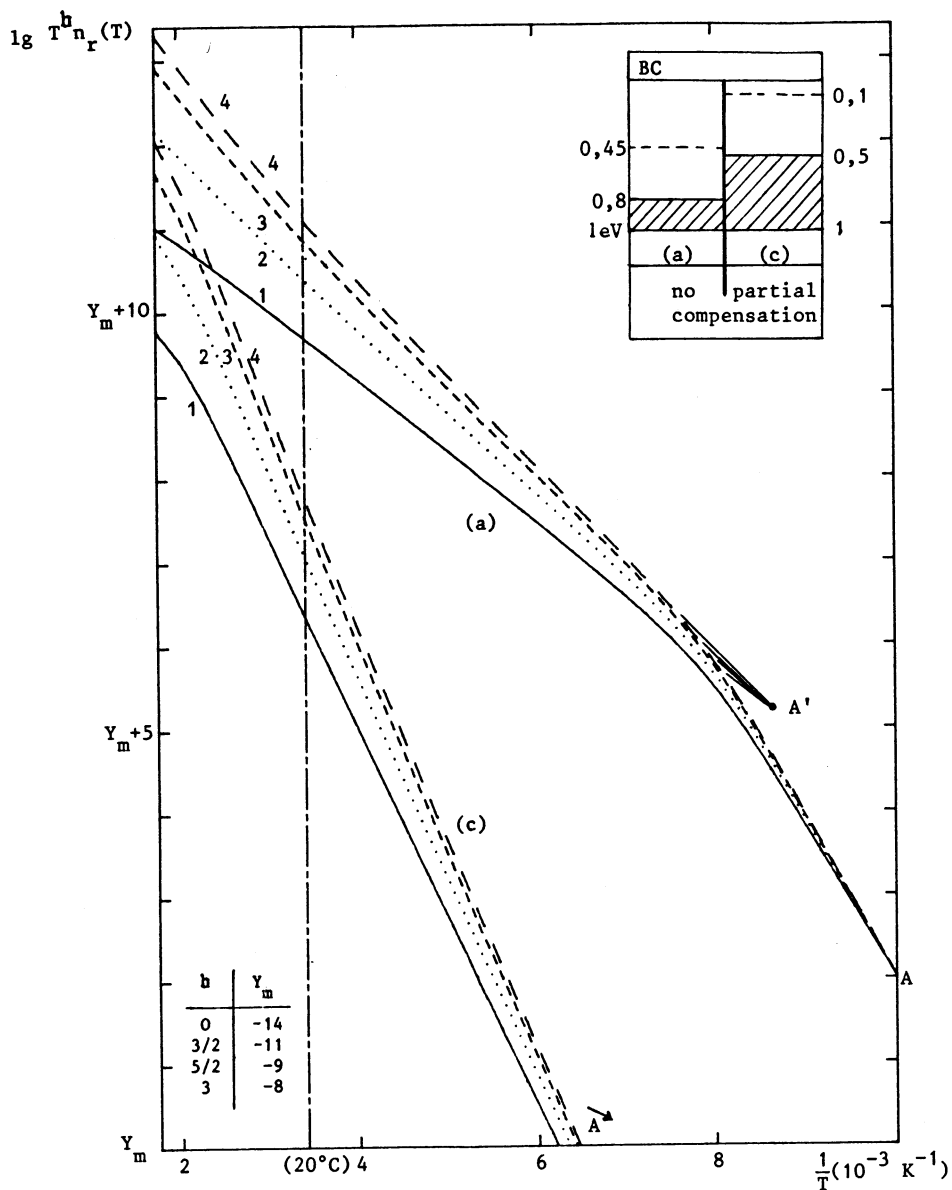


Fig. 4. — Variations of $\lg(n_r T^b)$ versus $1/T$ for a uniform band, and for different values of b . $\Phi_2 = 1$ eV. Type (a) curves: $s_{max} = 0.1$; $\delta\Phi = 0.2$ eV; $q = 10^7$; $\Delta\Phi_p/\Phi_2 = 0.45$. Type (c) curves: $s_{max} = 10^{-2}$; $\delta\Phi = 0.5$ eV; $q = 10.4$; $\Delta\Phi_p/\Phi_2 = 0.10$. (—) a_1, c_1 ; $b = 0$ (.....) a_2, c_2 ; $b = 3/2$. (- - - - -) a_3, c_3 ; $b = 5/2$ (— — —) a_4, c_4 ; $b = 3$.

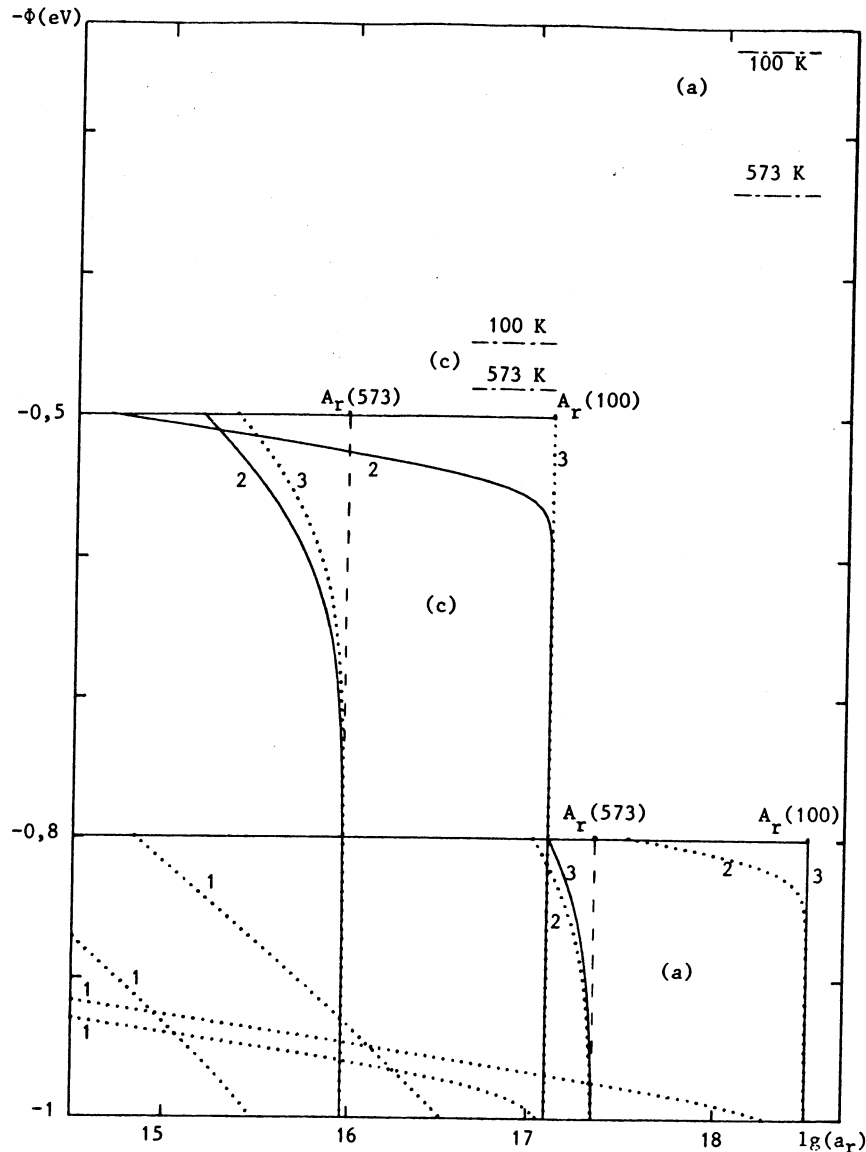


Fig. 5. — Variations of reduced densities a_r of electrons trapped in donor levels, in terms of their depth (with inverted signs to picture energy levels as usual) : (—) profiles (a) and (c) corresponding to conditions of curves (a) and (c) of figure 4 ; (---) quasi-Fermi level positions corresponding to these cases, at temperatures 100 K and 573 K ; (—) limits of $A_r(T)$; (.....) (a) - type and (c) - type profiles for complementary values of q : (1) 1.04 ; (2) 10.4 ; (3) 10^7 .

with $A_r = s/\delta\Phi$. Curves drawn in full line, give the profiles of level occupation, at 100 K and 573 K, corresponding respectively to the non-compensated (a)-type, and to the compensated (c)-type, cases. Figure 5 shows, mainly, that an increase in T results in a re-distribution of electrons amid the levels : the rate of occupation of deep levels is decreased, while that of shallower levels is increased. This originates both from the Fermi level shift indicated in the figure, and from the spreading with T of the Fermi distribution function. This pictures a very intricate interdependence of levels, which precludes a linear superposition of their contributions to the conductivity.

To widen a little more this approach, we investi-

gated the influence of q variations. Thus, we verified that quasi-linear curves are still obtained over extended ranges of T . Apparent site depths Φ deduced from curve slopes differ significantly from that of table I.

(iii) A lot of simulations, not reported in this paper, have been made to cover more general cases than those of figure 4. The only indication we want to give here, concerns the levelling off in the high temperature range, that was apparent on some curves in figures 1 to 3. When $\sigma(T) \propto n_r(T)$ is considered, instead of $\sigma(T) \propto T^{3/2} n_r(T)$, this plateau of saturation is replaced by an increasing portion, along which conductivity becomes a decreasing function of T , until a maximum is reached.

This somewhat surprising, metallic-conduction-like effect, is directly related to the existence of a saturation. For, in this zone, the density of free electrons is very close to its maximum, and is practically insensitive to temperature. Then, the observed decrease of $\sigma(T)$ proceeds readily from that of $\mu(T) \propto T^{-3/2}$. This effect extends over a larger interval, the smaller s_{\max} .

3.3 BAND MODEL INVESTIGATION WITH BOLTZMANN FUNCTION. — The preceding investigation, made only by computer simulation of equation (6) above, cannot bring easily physical insights into the observed behaviours. To attempt to do this, and to avoid overwhelming complexities, inherent to Fermi-Dirac statistics, we suppose here that suitable conditions are met, allowing for Boltzmann statistics to apply. Then, the relationship

$$dn_d = \frac{A_d d\Phi}{1 + n_r \exp(\eta - \alpha_p)}, \quad (7)$$

giving the density of electrons freed from a slab of width $d\Phi$, can take two approximate forms, depending on whether, on the interval (η_1, η_2) :

$$\text{or} \quad n_r \exp(\eta_1 - \alpha_p) \gg 1, \quad (8a)$$

$$n_r \exp(\eta_2 - \alpha_p) \ll 1. \quad (8b)$$

Condition (8a) can be achieved, only, for sufficiently low field strengths for which $\alpha_p < \eta_1$. For larger fields, (8a) must be inverted. Cases can then exist where an inversion of (8b) is simultaneously realized. This is not considered hereafter.

Integrating (7), both when conditions (8a) and (8b) apply, gives the respective solutions:

$$n_r = \frac{s}{2q} (\sqrt{1 + K(\alpha_p, T)} - 1) \quad (9a)$$

and

$$n_r = \frac{s \frac{q-1}{q}}{1 + e^{-\alpha_p} \langle e^\eta \rangle}. \quad (9b)$$

In these equations, $K(\alpha_p, T) = \frac{4q^2}{s} e^{\alpha_p} \langle e^{-\eta} \rangle$,

and

$$\langle e^{\pm \eta} \rangle = \frac{1}{\delta \eta} \int_{\eta_1}^{\eta_2} e^{\pm \eta} d\eta = \pm \frac{e^{\pm \eta_2} - e^{\pm \eta_1}}{\delta \eta}. \quad (10)$$

Now, let us compare equation (9a) with the relationship that holds when Boltzmann function applies to the single level case (Eq. (8a) of [9]).

$$n_r = \frac{s}{2q} \left(\sqrt{1 + \frac{4q^2}{s} e^{\alpha_p} e^{-\eta} - 1} \right). \quad (9c)$$

It appears that the two equations differ only through the substitution of $e^{-\eta}$ for $\langle e^{-\eta} \rangle$.

Equations (9) can be further simplified. Indeed, when the band widens, so that $\delta \Phi \gg kT$ over the full temperature range, equation (9a) reduces to:

$$n_r = q \frac{kT}{\delta \Phi} \exp(-\eta_1 + \alpha_p). \quad (11a)$$

For equation (9b), it can be remarked that $e^{-\alpha_p} \langle e^\eta \rangle \cong e^{\eta_2 - \alpha_p}$. Now $e^{\eta_2 - \alpha_p} \gg 1$ as long as the rate of saturation $\Delta \Phi_p / \Phi_2$ remains far below 1. This equation gives then:

$$n_r = s \frac{q-1}{q} \exp(-\eta_2 + \alpha_p). \quad (11b)$$

These equations show that, depending on which of the conditions (8) is fulfilled, either of the limits of a wide band can be found, in an Arrhenius plot. However, a large set of simulations showed us that (8b) seems practically the only available condition. In such a case, an apparent activation energy $*\Phi = 1$ eV was effectively deduced. But when other conditions were fulfilled, we obtained, as indicated partially in table I, either irrelevant values, or intermediate values, ranging amid the (Φ_1, Φ_2) interval.

These considerations show that Boltzmann distribution function is rarely available, when a band of donors is concerned. Anyway, as the existence of a band of donors remains experimentally hidden, no clear significance can be assigned to the energy values obtained in an Arrhenius plot. However, it was observed that, when a single level is concerned, the two possible exponential developments of equation (9c) can be convenient approaches, but over separate temperature ranges. Nevertheless, even in this case, an undetermination remains, in relation with the slope parameter value m . We postpone to sub-section 5 the remaining problem of interpreting the order in which the two slopes are liable to appear ($m = 2$ in the higher temperature range as for example in Fig. 3a).

4. Analysis of possible reasons for failure of the splittability principle.

4.1 DISTINCTION BETWEEN MATHEMATICAL AND PHYSICAL APPROACHES. — The proof of the Arrhenius plot inadequacy, in the investigation of localized levels in the gap, was supported, in the above developments, on computer simulations of some definite models. This process affords a convincing demonstration, but it presents two faint points: on the one hand, it does not have the full generality of a theorem, and does not preclude the existence of cases where the principle avails; and on the other hand, it does not allow a straightforward understanding of the possible origins of the failure of the splittability principle.

For the sake of conspicuousness, and to try to

generalize somewhat our results, it is essential to examine very carefully the subtending mechanisms over which this principle is founded.

Let us emphasize again that the Arrhenius representation has a well defined meaning, from a purely mathematical prospect. And that, consequently, any decomposition of continuous, oftentimes monotonically decreasing, functions, is fully legitimate. This makes clear that the failure of the Arrhenius diagrams, has a purely physical origin. In other words, since the bi-univocal slope-energy correspondence reveals erroneous, in our models, this means that the splittability principle must necessarily violate, at least, one of the underlying physical laws of the system.

Now, it can be shown, starting from a simple calculation, and with the help of computer simulation, that this principle fails, generally, in giving back occupation probabilities of localized levels, that can agree with Fermi-Dirac distribution function.

4.2 CONDITIONS FOR THE SPLITTABILITY OF TWO DONOR LEVELS.

4.2.1 Mathematical approach. — Consider, for instance, two donor levels lying at depths Φ_1 and Φ_2 ($\Phi_1 < \Phi_2$), with densities N_{d1} and N_{d2} . In addition, very deep lying acceptors are admitted, with density N_a . Then, Fermi-Dirac statistics gives, for the free electron relative density n_r , under a given applied field :

$$n_r + \frac{s}{q} = \frac{s_1}{1 + n_r \exp(\eta_1 - \alpha_p)} + \frac{s_2}{1 + n_r \exp(\eta_2 - \alpha_p)}, \quad (12)$$

with $\eta_i = \Phi_i/kT$, $s_i = N_{di}/N_c$; and $s = s_1 + s_2$.

In this equation, Boltzmann function is supposed to apply, as usual for non-degenerate conditions, for electrons in the conduction band. Equation (12) is a third degree polynomial in n_r . Its resulting analytical solution is too much awkward to avail (see, for example, Mahapatra and Roy, [19]). But this equation reduces either to a second order, or to a first order, polynomial, in proper limiting cases. When inequality (8a) is fulfilled, one obtains the solution :

$$n_r = \frac{s}{2q} \left(\sqrt{1 + \frac{4q^2}{s} \Lambda} - 1 \right) \quad (13a)$$

with

$$\Lambda = \frac{e^{-\eta_1 + \alpha_p}}{p} (1 + (p-1) e^{-\delta\eta}).$$

While inequality (8b) leads to the solution :

$$n_r = \frac{s \frac{q-1}{q}}{1 + \frac{s}{p} e^{\eta_1 - \alpha_p} (1 + (p-1) e^{\delta\eta})}. \quad (13b)$$

In these equations, $p = s/s_1$ is a parameter ≥ 1 , and $\delta\eta = (\Phi_2 - \Phi_1)/kT$ is the reduced distance apart the levels. As previously stated, equation (13a) is valid only for $\alpha_p < \eta_1$. It is worth noting the close forms of equations (9) and (13).

4.2.1.1 Application of inequality (8a). — The splittability principle does not apply directly to equation (13a), in general conditions. But it could be of interest to know whether its application should be possible when Λ is very smaller or very larger than 1. This happens respectively when $\Lambda \ll \frac{s}{4q^2} = N_a^2/4 N_c N_d < 1$, and when $\Lambda \gg \frac{s}{4q^2}$. Condition

$$\frac{4q^2}{s} \Lambda \gg 1 \quad (14a1)$$

would rather correspond to situations where the donor density, and/or compensation, are large. The splittability principle would then apply, for :

$$n_r = \sqrt{\frac{s}{p}} e^{\alpha_p/2} \sqrt{e^{-\eta_1} + (p-1) e^{-\eta_2}}. \quad (15a1)$$

But, the first member of equation (14a1) is an increasing function of T , and this condition cannot be fulfilled over extended intervals in T , especially in the low temperature range.

Condition

$$\frac{4q^2}{s} \Lambda \ll 1 \quad (14a2)$$

would rather correspond to weak donor densities, and/or poor compensation. It cannot, as a principle, be fulfilled in the high temperature range. The splittability principle should also apply to this case, for :

$$n_r = \frac{q}{p} e^{\alpha_p} (e^{-\eta_1} + (p-1) e^{-\eta_2}). \quad (15a2)$$

It appears at this stage, that an experimentalist, being generally unable to know which of the relationships (14a) would apply, cannot determine whether the energies, eventually found, must be affected or not by a factor 1/2. But, in addition, he can no more decide which of the conditions (8) is fulfilled. We observed, numerically, that inequalities (8a) and (14a1) do not seem to be often both compatible.

4.2.1.2 Application of inequality (8b). — In suitable conditions where relationship (8b) avails, equation

(13b) does apply. In the following, we consider only, among all possibilities of development of this equation, the most interesting cases, obtained when

$$\frac{s}{p} \exp(\eta_1 - \alpha_p) \gg 1. \quad (14b)$$

This condition gives immediately :

$$n_r = p \frac{q-1}{q} \frac{\exp(-\eta_1 + \alpha_p)}{1 + (p-1)e^{\delta\eta}}. \quad (15b)$$

Two more approximations can be made in equation (15b).

(i) When $\delta\eta$ is large enough, over a suitable temperature range, and provided that p does not approach closely 1,

$$(p-1)e^{\delta\eta} \gg 1. \quad (14b1)$$

Then, equation (15b) reduces to :

$$n_r = \frac{p}{p-1} \frac{q-1}{q} \exp(-\eta_2 + \alpha_p). \quad (15b1)$$

In these conditions, the deeper level, only, can be detected (compare to Eq. (11b)).

(ii) When $\delta\eta$ is small, and p approaches 1,

$$(p-1)e^{\delta\eta} \ll 1 \quad (14b2)$$

equation (15b) becomes :

$$n_r = p \frac{q-1}{q} \exp(-\eta_1 + \alpha_p). \quad (15b2)$$

Then, the shallow level is only found. But it must be emphasized that condition (14b2) refers, in fact, to a vanishing density of states for the deep level.

Finally, when inequation (8b) is liable to apply, the ultimate limiting forms of equation (12) correspond to applications of the splittability principle, where one of the two levels is shadowed.

4.2.2 Computational approach. — A large set of simulations was performed, in order to test and exemplify the conditions of validity of the various approximations introduced above. This was done in two directions. First, we tried to find conditions where the diverse limiting forms could work. Secondly, we tried to put forward, on a more general basis, a wealth of examples of effective curve shapings that can be obtained with two donor levels.

4.2.2.1 Examples using the limiting forms (2 variable parameters). — Curves drawn in figure 6a were chosen to allow a relatively straightforward correspondence of their shapes, with one of the aforementioned approximate equations. The levels are always lying at depths $\Phi_1 = 0.35$ eV and $\Phi_2 = 0.50$ eV, and their total relative density s_{max} is held constant.

The only modified parameters are the respective donor densities, through p , and the rate of compensation q . The applied field is constant and so low as to make $\Delta\Phi_p = 0.005$ eV, so that the present attainments become clearly independent of any PF effect. Results of simulations are tabulated in table II.

Table II.

Curve numbers	1	2	3	4	5	6	7	8
p	2	2	2	2	1.04	10.4	10^7	1.1
q	1.004	1.04	10.4	10^6	1.04	10.4	10^7	1.8
$*\Phi_{cv}$	0.50	0.50	0.35	0.16	0.42	0.43	0.24	0.35
				0.35			0.49	

Curves (1)-(3) are obtained with levels of equal densities ($p = 2$), and q amounting respectively to 1.004, 1.04, and 10.4. A unique activation energy is then found, equal to either Φ_2 or Φ_1 . Fitting of curves is then realized, with an excellent approximation, either by equation (15b1), or by equation (15a2) reduced to its first term. This exemplify the role played by compensation. When a nearly full compensation is achieved, level Φ_1 is completely empty, and thermal emptying of electrons remaining in level Φ_2 is only working. But with a lesser compensation, as in curve (3), level Φ_2 is completely filled, and thermal emptying is dealt only with the remaining electrons of level Φ_1 . Intermediate cases of compensation ($1.04 < q < 10.4$), liable to give both Φ_1 and Φ_2 , have not been investigated.

Curves (5)-(7) are obtained in the particular condition $p = q$, and with $q = 1.04$; 10.4 and 10^7 . The respective density weights are roughly inverted from curve (5) to curve (6). Inequalities (8) are both invalid, and must be inverted to give $n_r \exp(\eta_1 - \alpha_p) \ll 1$ and $n_r \exp(\eta_2 - \alpha_p) \gg 1$. The apparent activation energy $*\Phi$ lies then between Φ_1 and Φ_2 .

Curves (4) and (7), obtained respectively with levels of equal densities and with a very light level Φ_1 , correspond both to non-compensation cases ($q = 10^6$, and $q = 10^7$). Consequently, they display two slopes, as usual. But, only one activation energy $*\Phi$ (Φ_1 for curve (4), and Φ_2 for curve (7)) can be deduced from them, the high and low temperature ranges corresponding respectively to $m = 2$ and $m = 1$. For curve (4), for instance, this explains as follows. In the high temperature range, condition (14a1) is verified, and consequently, the related linear part of the curve obeys equation (15a1), with $(p-1)e^{-\delta\eta} \ll 1$. In the low temperature range, at the opposite, condition (14a2) applies, and

the corresponding linear part obeys equation (15a2), limited again to its first term.

For the sake of conspicuousness, we represented also, in figure 6b, the variations of $-\Phi_{F_n}$ versus T^{-1} corresponding to curves (1)-(8) of figure 6a. The two postulated levels were drawn in order to make more apparent the various $-\Phi_{F_n}$ relative positionings. In addition, we drew a second ordinate scaling visualizing, in each case, the $^*\Phi$ positions, labelled alike curves of figure 6a. Thus it is shown that, when one slope only is apparent on curves (curves (1), (2), (5) and (8)), $-\Phi_{F_n}$ moves steadily in direction of the level $^*\Phi$ effectively found, when

T is decreased. But when curves display two slopes, or nearby saturation, $-\Phi_{F_n}$ goes through a maximum (curves (3), (4), (6), (7)), transition of the slope parameter m from 1 to 2 occurring there. The following additional remarks can be made about the case of nearly full compensation for which two situations can be met. When densities of levels are of the same order of magnitude, Φ_2 is found because level Φ_1 is completely emptied by compensation (curves (1) and (2)). When the ratio of level densities is nearly equal to the compensation ratio q , the populations of levels are of the same order of magnitude, and $^*\Phi$ lies amid Φ_1 and Φ_2 . Crosses in

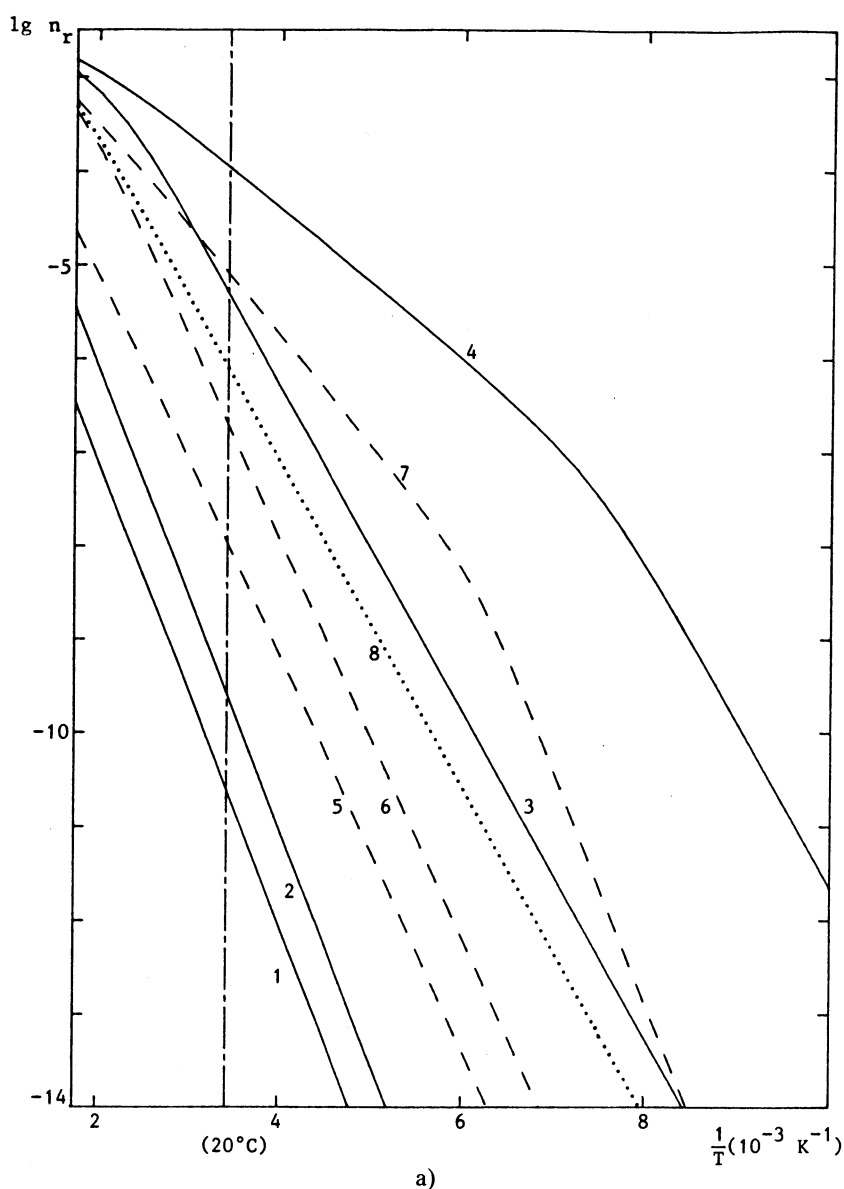


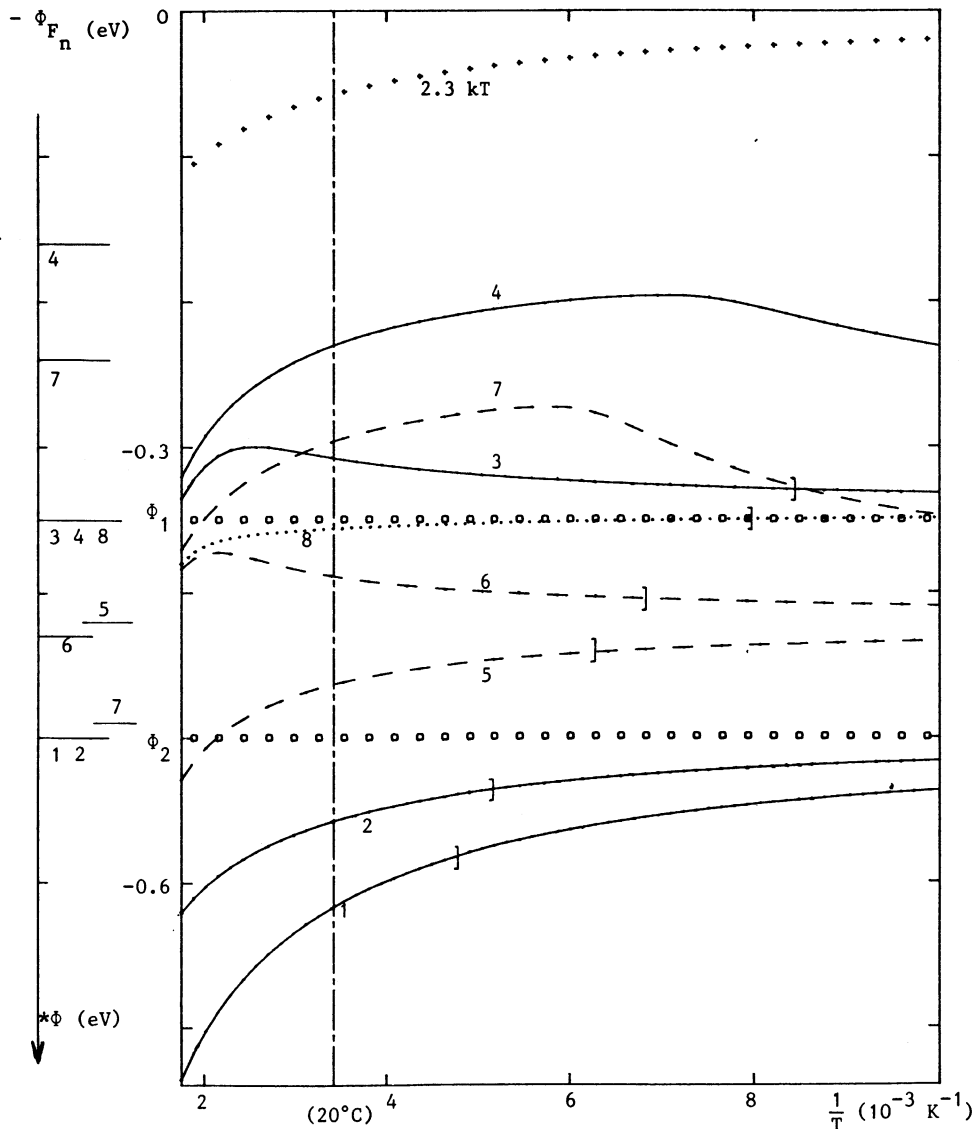
Fig. 6. — (a) Arrhenius diagrams of $n_r(T^{-1})$ for two single levels with varying respective densities, and for various compensation rates. $\Phi_1 = 0.35$ eV ; $\Phi_2 = 0.50$ eV ; $s_{\max} = 0.1$; $\Delta\Phi_p/\Phi_2 = 0.01$. (—) $p = 2$: (1) $q = 1.004$; (2) $q = 1.04$; (3) $q = 10.4$; (4) $q = 10^6$. (---) $p = q$: (5) $q = 1.04$; (6) $q = 10.4$; (7) $q = 10^7$. (.....) $p = 1.1$: (8) $q = 1.8$. (b) Fermi-level variations $-\Phi_{F_n} = E_{F_n} - E_c$ versus $1/T$ for curves of figure 6a. A second scaling gives the related $^*\Phi$ positions, labelled alike curves. Brackets delimit the related actual intervals of T used in figure 6a.

the figure indicate the $-2.3 kT$ departure from $-\Phi_{Fn}$, by which Fermi-Dirac function can be approximated by Boltzmann function within 10 %.

4.2.2.2 More general cases (all parameters allowed to vary). — Curves of figure 6a could incite to believe that the twin-level model should display a relatively simple behaviour, not very different from that of a band. However, it is easy to establish that, in general cases where all the parameters of the system are allowed to vary, the curve shapes, obtained in an Arrhenius plot, are not directly foreseeable. To show this, we have proceeded to a large simulation, where parameters s , p , q , Φ_1 , Φ_2 and α_p were modified. Only few trends are reported here just in order to emphasize further the difficulties pouring in from the analysis using the splittability principle. We mainly tried to make apparent the prominent differences, departing the present model from that of a uniform band.

Figure 7 gives some examples of curve shapes, obtained directly from equation (12). The respective positions of Φ_1 and Φ_2 are indicated in an inset in the figure. In every cases, a medium compensation is introduced ($q = 10$), and the applied field is always taken either low or moderate ($6.8 \times 10^4 \text{ V.m}^{-1} \cong F \cong 3.8 \times 10^6 \text{ V.m}^{-1}$, for a coulombic PF effect, and with $\epsilon = 2.2$). p is always lesser than q : $p = 9.5$ for curve (1), and $p = 9.9995$ for curves (2)-(4). This makes the density of level Φ_1 to amount to about 1/10th of the density of Φ_2 . $s_{\text{max}} = 0.1$.

The curves, represented in the figure, were chosen : on the one hand because of their shapes, more usual than those of figure 6a, in analyses using the splittability principle ; on the other hand to show that large variations of shapes can result from moderate modifications of few parameters only. Moreover, curve (3) presents the peculiarity of displaying an intermediate levelling, which can be



b)

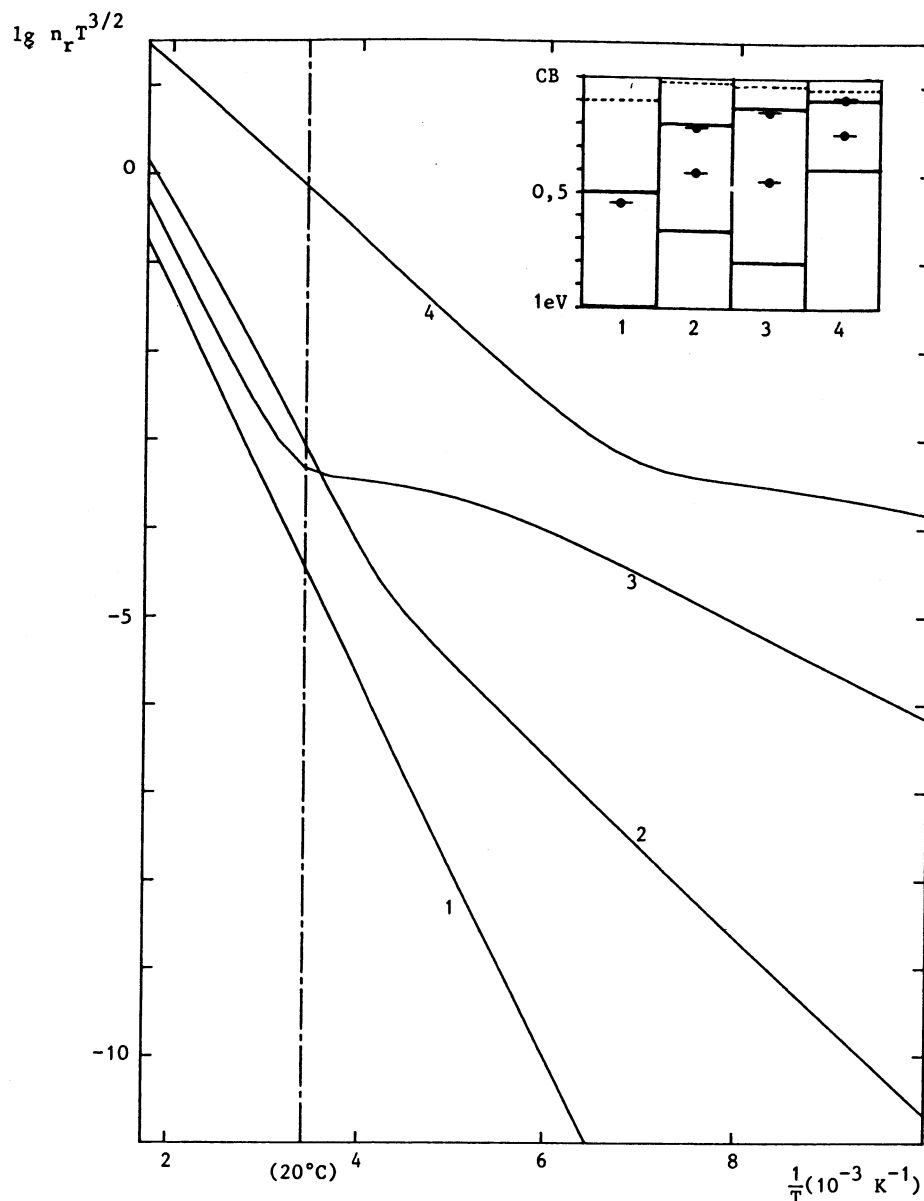


Fig. 7. — Arrhenius plot of $n_r T^{3/2}$ for two levels. $s_{\max} = 0.1$; $q = 10$. Curve (1): $p = 9.5$; curves (2)-(4): $p = 9.9995$. Other parameters are apparent in the caption: dashes indicate $\Delta\Phi_p$; (\bullet — \bullet) indicate $*\Phi$.

easily protracted towards high and low temperatures. Such a levelling is sometimes apparent in some experimental results, in the literature. Just in order to give one example, this can be found in a paper by Schmid [20], dealing with conductivity in glasses with various compositions. But the author, using the splittability principle, and hence Boltzmann function ordinarily associated with it, did not attempt to bring an interpretation to the observed plateaus.

Table III indicates the values of $*\Phi$, deduced graphically from figure 7. It is observed that, the shallow level is always approximately found, in the lower available temperature range. While the value calculated for the deep level, when apparently determinable, is always wrong.

Table III.

Curves	1	2	3	4
Φ_1 eV	0.500	0.200	0.135	0.100
Φ_2 eV	1.000	0.670	0.800	0.400
$\Delta\Phi_p$ eV	0.100	0.013	0.040	0.052
$*\Phi$ eV	0.536 —	0.215 0.407	0.148 0.444	0.086 0.244

This confirms once more that misleading interpretations can result from the splittability principle,

even when two single levels are concerned. Moreover, all the results above, obtained under a very weak field, apply alike when the potential wells are insensitive to the field. Therefore, it must be concluded that the failure of this principle is not strictly limited to PF and related effects, but has to be extended to any kind of flaws, distributed in the gap of solids.

To widen the present analysis, we have also initiated a study of a model including uniform distributions, shared among two separated bands. Such systems, involving two more parameters, allow to control independently the range of intermediate levelling and curve slopes as well.

4.3 POSITIONING OF OUR ANALYSIS WITH RESPECT TO FORMER WORKS. — As far as we know it, the essential of calculations made in [9] and [10] are original, even if some authors, like Connell *et al.*, have initiated a similar, but more restricted, approach. But equations like equation (6) are certainly not original. Effectively, many authors have, long ago, determined the densities of electrons in the conduction band, when a lot of discrete levels are postulated in the gap. This is the case, for example, for Shockley and Last [21]. A practically exhaustive account of such calculations was given, later, by Blakemore [22]. This author presents calculations corresponding to two kinds of discrete level distributions. In the first kind, the traps possess a single fundamental level, but, in addition, the trapped electrons may occupy excited levels. In the second kind of distribution, the traps are shared among a lot of fundamental levels, each level being, in addition, splitted into excited states. For the sake of generality, Blakemore affects to each, fundamental or excited level, a spin degeneracy factor g . No field-induced deformation of the potential of the wells, is considered.

When only one fundamental level is postulated, the equation for n_r , transcribed in our notations, writes :

$$n_r + \frac{s}{q} = \frac{s}{1 + \sum_{i=0}^{\infty} g_i^{-1} \exp\left(-\frac{\Phi_F - \Phi_i}{kT} + \frac{\Phi_i}{kT}\right)} \quad (16a)$$

In this equation $\Phi_i = \Phi - \delta\Phi_i$ stands for the depth of the excited level i , while Φ is the depth of the fundamental level ($\delta\Phi_0 = 0$). If the Fermi level Φ_F lies many kT below the conduction band edge, this equation can also be written :

$$n_r + \frac{s}{q} = \frac{s}{1 + n_r \sum_{i=0}^{\infty} g_i^{-1} \exp\left(\frac{\Phi - \delta\Phi_i}{kT}\right)} \quad (16b)$$

As a result, a second degree polynomial in n_r obtains, which solution is very close to equations (6a)

and (6b) of [9], under zero field condition. Following Blakemore (see Fig. 32-13 of the author, p. 145), accounting for the excited states results in a slight, but significant, damping of the curve in an Arrhenius plot ($\lg n_r, 1/T$), mainly sensitive in the high temperature range, and up to saturation.

When many fundamental levels are introduced, the equation for n_r becomes :

$$n_r + \frac{s}{q} = \sum_{j=1}^M \frac{s_j}{1 + n_r \sum_{i=0}^{\infty} g_{ji}^{-1} \exp\left(\frac{\Phi_{ji}}{kT}\right)} \quad (17)$$

in the simplest case, again, where the Fermi level is sufficiently far below the bottom of conduction band. Therefore, determination of n_r needs then to solve a $(M + 1)$ degree polynomial. However, when Boltzmann function applies, the appropriate reductions of equation (17) lead to solutions formally similar to equations (13).

The authors who dealt with multi-level models, did not apparently pay much attention to the underlying problem set by the experimental discrimination of the involved levels.

4.4 SPLITABILITY PRINCIPLE AND PROBABILITIES OF LEVEL OCCUPATION. — It is now necessary to investigate the reasons why the splittability principle generally fails. We believe that this comes essentially from the fact that, in equations (12), (16) and (17), as when integrating equation (3) of [10], the total density n_r of conduction electrons is present in each term of the discrete sums, as well as in the infinitesimal summation leading to equations (4) therein. The respective contribution to these sums, of either of the terms, is therefore dependent on the overall contribution of all the levels involved. As a result, the contributions of these levels to n_r cannot generally be considered as independent, contrary to the requirement of the splittability principle. Besides, the interdependence of populations of different levels was already illustrated in figure 5, dealing with a uniform distribution. This figure shows clearly that a rise in temperature results in a re-distribution of electrons among the various levels. The deeper levels are always progressively emptied. But the populations of upper levels do not vary so monotonically, at least when compensation is not too weak. While some are always emptying, others, located nearby the upper limit of the band, can be partially replenished. This comes both from a shift of the Fermi level, and from a widening of the range of variation of the Fermi function. As a result, Fermi-Dirac statistics leads, generally, to situations where the response of the system is very involved, and cannot be analyzed as a sum of independent terms.

Conversely, let us suppose independent the contributions of the two levels, to the density of conduction

electrons. This density can then be written, using the detailed balance principle :

$$n + N_a = n_1(N_{d1}, \Phi_1) + n_2(N_{d2}, \Phi_2).$$

Now, if the populations of the two levels are still supposed to be describable by a, presently undetermined, distribution function f , and if the concept of Fermi level is preserved, it can also be stated that :

$$\begin{aligned} n_1 &= N_{d1} f(\Phi_1, \Phi_F, N_a) \\ n_2 &= N_{d2} f(\Phi_2, \Phi_F, N_a). \end{aligned}$$

Then, resolving these equations with respect to Φ_F gives :

$$\begin{aligned} (\Phi_F)_1 &= g(n_1, N_{d1}, \Phi_1, N_a) \\ (\Phi_F)_2 &= g(n_2, N_{d2}, \Phi_2, N_a). \end{aligned}$$

Therefore two differing values of Φ_F are then found, for any sets of arbitrary values of the involved, independent, parameters. Thus, the assumption of level independence, results generally in a non-uniqueness of the Fermi level.

Hence, the assertion of a general availability, for the splittability principle, would entail a disbelief of the notion of Fermi energy. Oppositely, the Boltzmann distribution function would always avail, as it does not resort to any reference level. Therefore, we believe to have established that, in data plots inferring the splittability principle, one must kept in mind that no reliability is provided by such plots, in themselves, concerning the determination of the involved parameters.

5. Conclusion.

It was observed, along the present study, that the behaviour of a model of donors distributed uniformly within a band, offers generally less diversity than a model involving two discrete levels. Among the discrepancies, a prominent one is particularly noticeable, as it offers an opportunity of setting an interesting problem of methodological analysis.

When a model, involving either a band or one level only, is adopted, two linear portions are liable to appear in an Arrhenius plot. But then, we observed that the less steeper line corresponds always to the high temperature range. The same situation can also hold when two levels are concerned, as shown by figure 6a. But with this latter model, it is also possible to observe an inversion of the two linear parts (Fig. 7), with the steeper one located in the high temperature range, a situation very commonly found in literature.

When slope steepness is increasing with temperature, the splittability principle does not give rise to difficulties in interpretations. For, then, energy levels are readily deduced from the slope magni-

tudes. But, in the opposite case of decreasing steepness, the bi-univocal slope-energy correspondence can no more be used, without introducing, at least, an additional assumption.

Our models could then provide an alternative explanation of such kinds of behaviour. But, as we showed that Arrhenius plots fail generally in giving faithful informations, about either trap depths or local density of states, we should not attempt to assign any precise meaning to the activation energies found experimentally. Having put forward that the splittability principle entails some invalidation of Fermi-Dirac statistics, we incline to believe that the unavailability of this principle should extend far beyond the models on which it was established. We think peculiarly that this failure could encompass, more generally, all experiments interpretable with the help of a steady-state Fermi level, as for instance in photoconductivity measurements. However, even if our results did not enjoy such a generality, they have, at least, introduced some suspicion about the actual capability of the Arrhenius plot, as an available tool for localized level investigations. This should incite searchers, each in their own field, to examine critically whether they are allowed to use this tool. Particularly, a thorough re-examination seems desirable in the field of amorphous materials, where no refined general theory exists presently. This is needed especially as the existing models of distribution of localized levels, in the gap of those materials, are often supported by experimental analyses founded on the splittability principle. Nevertheless, it could be considered that a validation of these models, would be obtained by cross-checking with the results of other methods of measurement. But cross-checking is conclusive only if these methods do not lie on similar approximations. For, then, reciprocal compatibility would prove no more than self-consistency.

Finally, the above study, associated with extended simulations, showed that a rigorous treatment of models commonly used in Solid State Physics, could bring some renewal on different prospects.

(i) It leads, sometimes, to important deepening about the role played by the fundamental underlying hypotheses. (ii) As a consequence, it can result in a suspicion about the effectiveness of some basic concepts, usually admitted as rationally founded, even when being, actually, based upon common sense considerations. (iii) It can lead also to a questioning about the availability of certain methods of analysis of experimental data. (iv) And consequently, it can succeed in accessing to a new approach of the problems set by the interpretation of experiments.

However, insofar as we do not offer an alternative method of analysis of experimental data, a somewhat

pessimistic vision emerges from our work. Fortunately, it seems that the fact of being unable to characterize the actual localized level distributions in energy, is not a redhibitory hindrance of knowledge improvement, at least on the level of technological efficiency. Besides, this remark is directly related to the manner in which some authors, like Rose [23] and Lampert [24], consider the first approach of a

number of physical problems. These authors devoted many skilful conceptual manipulations, to show that the use of well-behaved ideas, connected with very simple formulations, could be a powerful tool in accessing, in a first step, to a convenient theoretical knowledge, of the response of materials to some kind of excitation. Nevertheless, the further step of thorough analysis, remains an essential requirement.

References

- [1] MOTT N. F., DAVIS E. A., Electronic processes in non-crystalline materials (Clarendon Press, Oxford) 1971.
 - [2] GARDNER D. G., GARDNER J. C., LAUSH G., MEINKE W. W., *J. Chem. Phys.* **31** (1959) 978-86.
 - [3] PROVENCHER S. W., *J. Chem. Phys.* **64** (1976) 2772-7.
 - [4] FRITZSCHE H., *J. Phys. Chem. Solids* **6** (1958) 69-79.
 - [5] FELIX M. C., FORNAZERO J., MACKOVSKI J. M., ONGARO R., *Revue Phys. Appl.* **15** (1980) 37-43.
 - [6] FELIX-VANDORPE M. C., MAITROT M., ONGARO R., *J. Phys. D.; Appl. Phys.* **18** (1985) 1385-99.
 - [7] COHEN M. H., FRITZSCHE H., OVSHINSKY S. R., *Phys. Rev. Lett.* **22** (1969) 1065-8.
 - [8] DAVIS E. A., MOTT N. F., *Philos. Mag.* **22** (1970) 903-22.
 - [9] ONGARO R., PILLONNET A., *Revue Phys. Appl.* **24** (1989) 1085.
 - [10] ONGARO R., PILLONNET A., *Revue Phys. Appl.* **24** (1989) 1097.
 - [11] CONWELL E. M., High field transport in semiconductors (Academic Press. N.Y.) 1967.
 - [12] RODE D. L., Semiconductors and semimetals (Academic Press, N.Y.) 1975.
 - [13] MOTT N. F., *Philos. Mag.* **19** (1969) 835-52.
 - [14] HOWARD D. J., SONDEHEIMER E. H., *Proc. Roy. Soc. London A* **219** (1953) 53-74.
 - [15] HOLSTEIN T., *Phys. Rev.* **124** (1961) 1329-47.
 - [16] BUBE R., Photoconductivity of solids (John Wiley and Sons, New York) 1960.
 - [17] STUKE J., *J. Non-cryst. Solids* **4** (1970) 1-26.
 - [18] CONNELL G. A. N., CAMPHAUSEN D. L., PAUL W., *Philos. Mag.* **26** (1972) 541-51.
 - [19] MAHAPATRA P. K., ROY C. L., *J. Phys. C.; Solid state phys.* **18** (1985) 3467-81.
 - [20] SCHMID A. P., *J. Appl. Phys.* **39** (1968) 3140-9.
 - [21] SHOCKLEY W., LAST J. T., *Phys. Rev.* **107** (1957) 392-6.
 - [22] BLAKEMORE J. S., International series of monographs on semiconductors, Vol. 3, Semiconductor statistics (Pergamon Press. Oxford) 1962.
 - [23] ROSE A., *RCA Rev.* **12** (1951) 362-414.
 - [24] LAMPERT M. A., *Phys. Rev.* **125** (1962) 126-41.
-